Available online at www.sciencedirect.com
ScienceDirect
Polymer 48 (2007) 5979–5987
polymer
www.elsevier.com/locate/polymer

Holographic polymer dispersed liquid crystals (HPDLCs) containing triallyl isocyanurate monomer

Timothy J. White [a,1], Lalgudi V. Natarajan [b], Vincent P. Tondiglia [b], Pamela F. Lloyd [c], Timothy J. Bunning [d,*], C. Allan Guymon [a,**]

[a] University of Iowa, Department of Chemical and Biochemical Engineering, Iowa City, IA 52242, USA
[b] Science Applications International Corporation (SAIC), Dayton, OH 45431, USA
[c] UES Inc., Dayton, OH 45432, USA
[d] Air Force Research Labs (AFRL), Wright Patterson Air Force Base, OH 45433, USA

Received 8 May 2007; received in revised form 1 August 2007; accepted 2 August 2007
Available online 8 August 2007

Abstract

The morphology and corresponding performance of holographic polymer dispersed liquid crystals (HPDLCs) based on thiol–ene polymer are dependent on a number of factors including the gel point conversion of the polymer, polymerization kinetics, and extent of liquid crystal (LC) phase separation. Previous research of HPDLC reflection gratings made from thiol–allyl ether polymer indicates that increasing polymerization rate in systems with moderate gel point conversion can improve diffraction efficiency (DE). This work examines HPDLC reflection gratings that contain the ene monomer triallyl isocyanurate (TATATO). In HPDLCs, thiol–TATATO polymerization is two times faster than the thiol–ene polymerization of triallyl ether. By substituting TATATO for triallyl ether, the LC droplet size within HPDLC reflection gratings decreases from 100 nm to 25 nm. The dramatic reduction in LC droplet size for thiol–TATATO HPDLCs increases baseline transmission from 55% in thiol–triallyl ether HPDLCs to 90% at 450 nm. Unfortunately, the DE of thiol–TATATO HPDLCs is only approximately 10% due to poorly defined lamellae in the grating morphology. As determined with real-time IR (RTIR) spectroscopy, thiol–TATATO HPDLCs have significantly faster LC demixing kinetics in comparison to thiol–allyl ether HPDLCs. During holographic photopolymerization, the increased rate of LC demixing causes formation of LC droplets throughout the grating. The low DE of thiol–TATATO HPDLCs can be improved by mixing TATATO and allyl ether monomer. The morphology of ternary thiol–ene HPDLC formulations containing TATATO and allyl ether has a well-defined grating structure due to increased LC solubility in the system, an average LC droplet size of 50 nm, and baseline transmission of nearly 85% at 450 nm.

Keywords: Holographic polymer dispersed liquid crystal (HPDLC); Polymerization kinetics; Liquid crystal phase separation

1. Introduction

Holographic polymer dispersed liquid crystals (HPDLCs) are promising materials with switchable diffractive capabilities useful in optical systems [1–4]. HPDLCs are formed through holographic illumination of a photoreactive mixture containing photoinitiator, monomer, and liquid crystal (LC). Upon illumination, the photoinitiator absorbs light, forms radicals, and initiates polymerization (photopolymerization) [5]. Since the rate of photopolymerization is a direct function of light intensity [6], monomer consumption is much faster in the regions of high light intensity, subsequently causing the formation of concentration gradients that disturb the equilibrium of the developing system. In an attempt to maintain equilibrium as monomer is consumed, monomer diffuses from the dark

* Corresponding author. Tel.: +1 937 255 9649; fax: +1 937 255 1128.
** Corresponding author. Tel.: +1 319 335 5015; fax: +1 319 335 1415.
E-mail addresses: timothy.bunning@wpafb.af.mil (T.J. Bunning), allan-guymon@uiowa.edu (C.A. Guymon).
[1] Present address: General Dynamics Information Technology (GDIT), Dayton, OH 45431, USA.

0032-3861/$ - see front matter © 2007 Elsevier Ltd. All rights reserved.
doi:10.1016/j.polymer.2007.08.007

regions into the light regions and nonreactive LC diffuses from the light regions to the dark regions. The result is a morphology consisting of alternating lamellae of polymer-rich and LC droplet-rich regions.

The use of acrylate-based HPDLCs in a wide range of applications has been limited by degradation and less than desirable optical performance [7,8]. On the other hand, HPDLCs formed in thiol–ene polymer have recently shown stable device performance for up to three years [9]. The optical performance of thiol–ene based HPDLCs also shows additional improvement over acrylate-based precursors in the fabrication of reflection gratings with uniform notch shape, improved performance consistency, increased diffraction efficiency (DE), and in some cases, reduced switching voltage (SV) [7,10,11]. Initial reports of thiol–ene based HPDLCs have utilized the commercial mixture NOA65 (Norland Products) [12], a common host matrix for polymer/LC composites [13]. Efficient reflection gratings have been formed across the visible spectra using the 365 nm line of a high power Argon-ion (Ar^+) laser and a prism. Unfortunately, the fabrication of high DE reflection gratings in the IR with UV-initiated holographic photopolymerization is not possible using prism holography. These optical constraints have been overcome with the development of visible photoinitiation systems that efficiently initiate thiol–ene photopolymerization using laser wavelengths of up to 647 nm [10,14]. Recently, Natarajan et al. used visible photoinitiation to fabricate HPDLC diffraction gratings in thiol–ene polymer with reflection notches at wavelengths as high as 1500 nm [10].

Despite the enhancements associated with the use of thiol–ene chemistry in HPDLCs, further improvement in electro-optical performance is desirable. Some of the critical factors necessary for generation of high performance thiol–ene HPDLCs have recently been documented [11,15]. These reports examine the impact of light intensity, ene monomer functionality, thiol monomer functionality, and thiol–ene stoichiometry on the development of thiol–ene based HPDLCs through characterization of polymerization kinetics, LC phase separation, polymer/LC morphology, and electro-optic performance. Both increasing polymerization rate and decreasing gel point conversion by increasing monomer functionality reduce LC droplet size and the extent of LC phase separation. However, HPDLC reflection gratings formed in thiol–ene systems with gel point conversion less than 40% have poorly defined polymer and LC lamellae that impart undesirable scattering and, subsequently, lower baseline transmission. HPDLC reflection gratings formed in thiol–ene systems with gel point conversion greater than 60% have large LC droplets that also scatter light and reduce baseline transmission. Therefore, thiol–ene HPDLC reflection gratings with fast polymerization rate and moderate polymer gel point conversion (40–60% conversion) yield the optimal combination of well-defined grating morphology and small LC droplets necessary for high baseline transmission and overall DE.

Thiol–ene polymerization kinetics are dependent on the structure of the thiol and ene monomers. Thiol–ene polymerization with mercaptopropionate thiol monomers is faster than with mercaptoacetate or aliphatic thiol monomers as thiyl radicals are stabilized by the ability of mercaptopropionate monomer to form a six-membered ring through hydrogen bonding [16,17]. The thiol–ene polymerization of vinyl (ene) monomer is dependent on electron density of the double bond [17,18]. Ene monomers with high electron density such as vinyl ethers, and triallyl isocyanurate (TATATO) exhibit rapid rates of thiol–ene polymerization. Based on these faster polymerization rates, PDLCs containing vinyl ether or TATATO monomer have smaller LC droplets in comparison to slower polymerizing thiol–allyl ether systems such as NOA65 [15,19,20].

This work examines the impact of polymerization behavior on LC phase separation, morphology, and performance of HPDLCs made from thiol–ene polymerizations with a particular focus on fast-reacting systems containing TATATO. HPDLC diffraction gratings were created to reflect green light (540–555 nm) by holographic interference of the 365 nm line of an Ar^+ laser. The influence of TATATO on the polymerization kinetics and LC phase separation was examined with real-time IR spectroscopy. The electro-optical performance of HPDLC reflection gratings was characterized with transmission spectroscopy. The performance of HPDLC reflection gratings was correlated to polymer/LC morphology as characterized by transmission electron microscopy (TEM).

2. Materials and methods

HPDLCs were formulated with 2 wt% of the UV photoinitiator Darocur 4265 (DC-4265, Ciba), 27 wt% of the liquid crystal BL037 (EMD Chemical), and 71 wt% of stoichiometric mixtures of thiol and ene monomer. BL037 is an eutectic mixture of cyano-*n*-phenyl compounds with a nematic to isotropic transition at 109 °C, positive dielectric anisotropy, an ordinary refractive index of 1.5260, and optical anisotropy (Δn) of 0.2820 [21]. All thiol–ene polymerizations in this report incorporate the trifunctional thiol monomer trimethylolpropane tris(3-mercaptopropionate) (trithiol, Aldrich). Difunctional ene monomers examined are trimethylolpropane diallyl ether (diallyl ether, Aldrich) and tri(ethylene glycol) divinyl ether (divinyl ether, Aldrich). The theoretical gel point conversion for the stoichiometric trithiol–diene mixtures is 71%. Trifunctional ene monomers were also examined, namely, pentaerythritol allyl ether (triallyl ether, Aldrich) and triallyl isocyanurate (TATATO, Aldrich). The theoretical gel point conversion of stoichiometric trithiol–triene mixtures is 50%. HPDLCs containing NOA65 (Norland Products) were also examined. Chemical structures for the monomers used in this study are shown in Fig. 1.

HPDLC reflection gratings were fabricated to diffract green light (540–555 nm) by holographic exposure with the 365 nm line of an Argon-ion (Ar^+) laser (Coherent, model 308c). The interference of the object and reference beams was induced using a single expanded beam and an isosceles 90° glass prism [7,10]. Glass spheres (10 μm) were added to the formulations to control grating thickness. Both conventional glass and

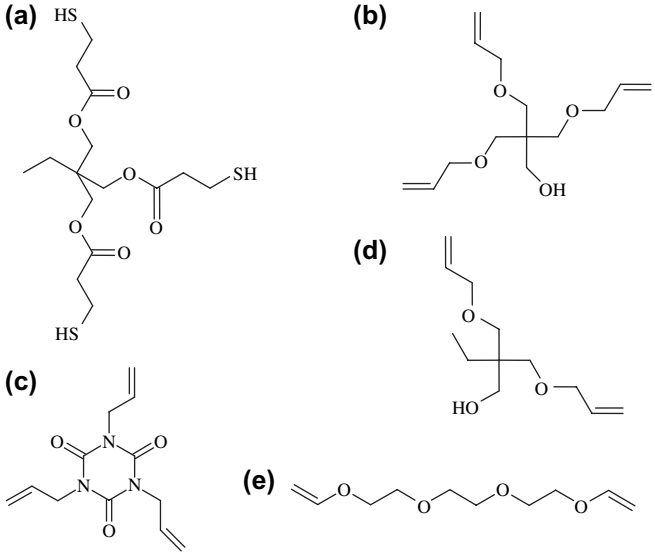

Fig. 1. Chemical structures of monomers used in this study. (a) Trithiol, (b) triallyl ether, (c) TATATO, (d) diallyl ether, and (e) divinyl ether.

indium-tin-oxide coated glass slides were used. Samples were holographically exposed for 1 min to form the HPDLC.

The diffraction efficiency (DE) and switching voltage (SV) of the fabricated HPDLC reflection gratings were characterized to gauge electro-optic performance. Both DE and SV were determined using an optical apparatus consisting of a white light source, a fiber optic spectrometer (Ocean Optics), an oscilloscope, and an amplifier. In this report, the DE is experimentally determined from the transmission spectra of a fabricated HPDLC reflection grating. The DE is calculated as the difference in transmission at the center of the reflection notch from the baseline to the peak of the reflection notch. The baseline is determined by fitting the spectra with a four parameter differential equation which is then directly compared to the actual transmission spectra. The switching characteristics of HPDLC reflection gratings are studied by examining the optical behavior of the grating with increasing voltage. Voltage was increased stepwise with an amplifier (square wave, 1 kHz, 5 V RMS) until DE approached 0%.

Polymer/LC morphology was imaged with transmission electron microscopy (TEM). HPDLC films were embedded in flat molds with a low viscosity TEM resin (Epo-fix) and polymerized overnight at 60 °C. After epoxidation, samples were ultramicrotomed (RMC PowerTome XL) with a 35° diamond knife (Diatome) at a thickness of 60 nm. These sections were vapor stained with RuO_4 to improve contrast and stability under the electron beam. HPDLC sections were imaged with a transmission electron microscope (FEI CM200) at 200 kV.

Polymerization rate and LC phase separation were examined with real-time IR (RTIR) spectroscopy. An FTIR spectrometer (Thermo Electron, Nexus 670) with liquid nitrogen cooled MCT detector was adapted to allow real-time examination of photopolymerization, as reported elsewhere [15,22]. Polymerization behavior of thiol and ene functional groups was examined at the S–H stretching peak at 2569 cm^{-1} and the =C–H stretching peak at 3078 cm^{-1}. Monomer conversion was determined during polymerization by monitoring the decrease in peak height absorbance. The polymerization rate was calculated by taking the time derivative of the functional group conversion. RTIR was also used to examine LC phase separation, by monitoring the appearance of the nematic phase of BL037. The amount of LC in the nematic phase (nematic fraction) was calculated from the peak height change of the cyano moiety at 2225 cm^{-1} [23]. The demixing kinetics (rate of nematic appearance) are examined by taking the time derivative of the normalized cyano absorbance. The use of RTIR to monitor LC phase separation has been described elsewhere in greater detail [15,22,24,25].

3. Results and discussion

The kinetics of thiol–ene polymerization are a direct function of the electron density of the double bond of the ene monomer. Double bonds with greater electron density react more quickly with thiyl radicals through chain transfer [17,18]. To illustrate the substantial influence of ene monomer on the polymerization kinetics of HPDLC formulations, Fig. 2 plots the polymerization rate for mixtures of trimethylolpropane tris(3-mercaptopropionate) (trithiol) with triethylene glycol divinyl ether (divinyl ether), TATATO, trimethylolpropane diallyl ether (diallyl ether), and pentaerythritol allyl ether (triallyl ether). The rate of polymerization was calculated from the time derivative of the fractional conversion of the ene monomer as determined by real-time IR (RTIR). As shown in Fig. 2, the thiol–ene polymerization of HPDLC formulations containing divinyl ether and TATATO is nearly two times faster than the rate of polymerization of the allyl ether monomers with equivalent functionality. Each of the thiol–ene polymerizations, regardless of the composition or functionality of the ene monomer, approaches 100% conversion. The fastest polymerization rate for these systems is evident in thiol–TATATO polymerization which is approximately 40% faster than thiol–divinyl ether polymerization.

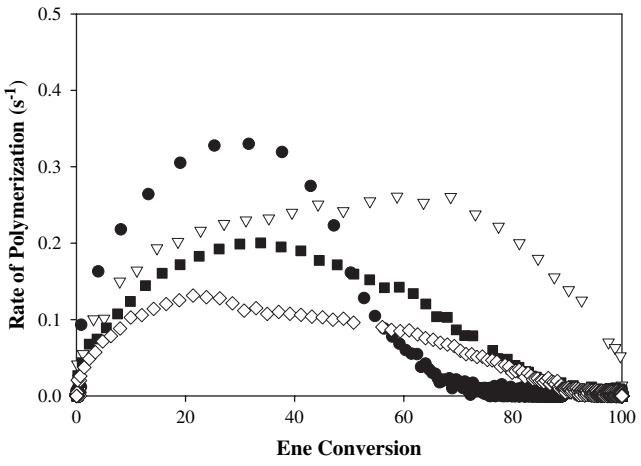

Fig. 2. RTIR determination of rate of polymerization (ene) versus ene conversion for polymerization of HPDLC formulations containing TATATO (●), divinyl ether (▽), triallyl ether (■), and diallyl ether (◇).

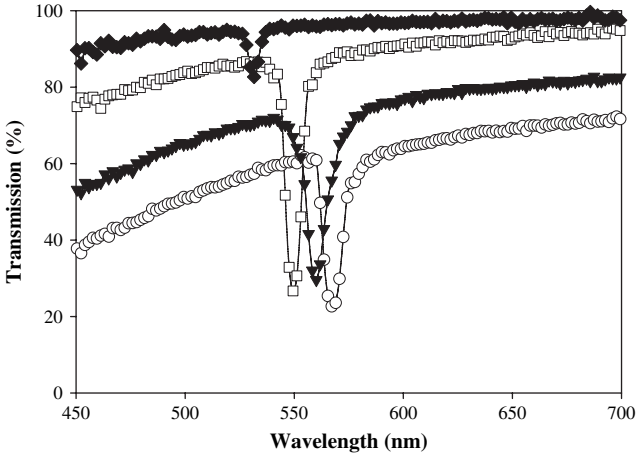

Fig. 3. Transmission spectra of HPDLC reflection gratings formed from polymerization of trithiol with TATATO (◆), divinyl ether (□), triallyl ether (▼), and diallyl ether (○). Laser intensity – 60 mW/cm^2.

Previous HPDLC research has shown that baseline transmission and overall DE strongly depend on polymerization rate [11]. The impact of faster-reacting ene monomer on performance is shown through comparison of HPDLC reflection gratings based on the polymerization of trithiol with diallyl ether, triallyl ether, divinyl ether, and TATATO. As evident in Fig. 3, the transmission spectra of HPDLC systems based on TATATO and divinyl ether have much higher baseline transmission than reflection gratings formed from allyl ether monomers of equivalent functionality. Baseline transmission, which can be illustrated by comparing the transmission at 450 nm for the gratings, is less than 40% in the diallyl ether system and slightly greater than 50% in the triallyl ether system. Replacing allyl ether monomer with divinyl ether or TATATO significantly increases transmission at 450 nm to approximately 80% and 90%, respectively. Baseline transmission is reduced by scattering losses as light travels through large LC droplets or poorly defined polymer and LC lamellae. Unfortunately, despite the enhancement in baseline transmission, HPDLCs based on TATATO have a DE of only 10%. HPDLCs formed by thiol–ene polymerization of divinyl ether have a DE of nearly 70%. These results indicate that fast-reacting ene monomers serve to increase baseline transmission but do not directly translate to the formation of high DE HPDLC reflection gratings.

The interesting optical properties of thiol–TATATO HPDLCs are likely dictated by the polymer/LC morphology which has been characterized with transmission electron microscopy (TEM). Fig. 4 contrasts the morphology of HPDLC reflection gratings formed from thiol–triallyl ether (a) and thiol–TATATO (b). Comparing the micrographs in Fig. 4a and b, it is evident that the ene monomer can impart significant changes to LC droplet size and grating morphology. The increased polymerization rate when triallyl ether is replaced with TATATO decreases LC droplet size from 100 nm to approximately 25 nm. The 25 nm LC droplets minimize light scattering and correspondingly increase the baseline transmission of HPDLC reflection gratings based on TATATO. Despite the small LC droplets, the DE of thiol–ene HPDLCs based on TATATO is poor. The polymer and LC lamellae in HPDLC reflection gratings based on TATATO are poorly defined. While LC droplets are more concentrated in the LC lamellae, a significant number of LC droplets are also present in the polymer lamellae. Therefore, the poorly defined lamellae in the morphology of thiol–TATATO HPDLC reflection gratings reduce DE by minimizing the refractive index mismatch between the polymer and LC regions.

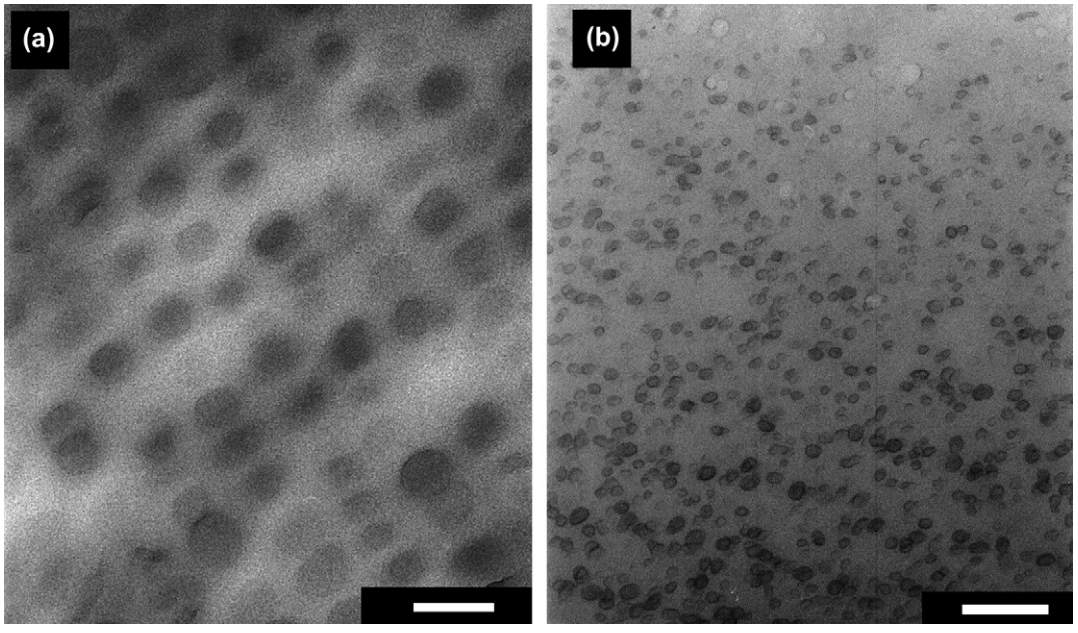

Fig. 4. TEM examination of polymer/LC morphology in HPDLC reflection gratings from polymerization of trithiol with (a) triallyl ether and (b) TATATO. Scale bar is 200 nm.

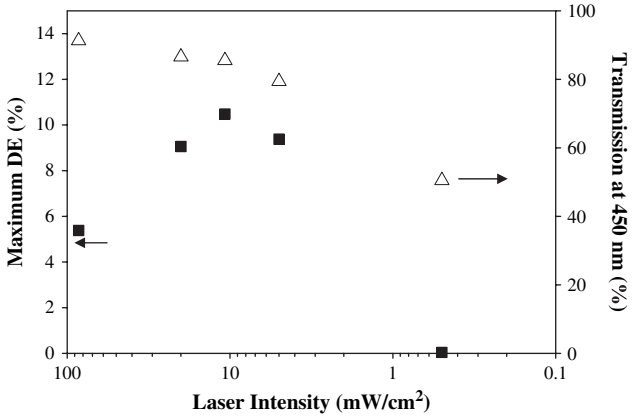

Fig. 5. Maximum DE (%) (■) and transmission at 450 nm (%) (△) for an HPDLC reflection grating based on TATATO polymerized at 0.5–85 mW/cm^2 of laser intensity.

To determine if the fast polymerization kinetics of thiol–TATATO systems are also the source of the poorly defined grating morphology, trithiol–TATATO HPDLC reflection gratings were fabricated over a range of laser intensity from 0.5 mW/cm^2 to 85 mW/cm^2. Reducing laser intensity decreases the rate of photopolymerization [5] and therefore, is a route to determine the impact of thiol–TATATO polymerization kinetics on DE in HPDLC systems. Fig. 5 plots DE and transmission at 450 nm against laser intensity. The DE of trithiol–TATATO HPDLC reflection gratings is only 5% when the laser intensity is 85 mW/cm^2. Decreasing the laser intensity slightly increases DE to a maximum value of 12% at 10 mW/cm^2. Baseline transmission is a direct function of laser intensity. HPDLCs polymerized with 85 mW/cm^2 have a baseline transmission of greater than 90% at 450 nm. As laser intensity is decreased, baseline transmission substantially decreases. The decreased transmission in HPDLCs polymerized with lower laser intensity is attributed to increasing LC droplet size. Clearly, the reflection notch of trithiol–TATATO HPDLCs is poor regardless of laser intensity.

Previous work has shown that performance of HPDLC can also be impacted by the kinetics of the LC phase separation process [26]. A number of variables are known to influence the evolution and extent of LC phase separation in thiol–ene based PDLC materials including light intensity (polymerization rate), gel point conversion, presence of excess monomer, and LC solubility [15]. In addition to quantifying the polymerization behavior of thiol–ene HPDLC formulations, RTIR is also an indirect means to monitor the evolution and extent of LC phase separation [15,22,24,25]. Since the IR absorbance of cyano-containing LCs such as BL037 is mesophase dependent, the amount of LC in the nematic phase (i.e. the nematic fraction) can be monitored during polymerization [27]. To quantify the impact of TATATO on LC phase separation, the nematic fraction of mixtures containing TATATO with diallyl ether is examined in Fig. 6a. The sample with the highest nematic fraction, and therefore, the greatest LC phase separation is that containing 100% TATATO monomer. As TATATO concentration is reduced, the nematic fraction

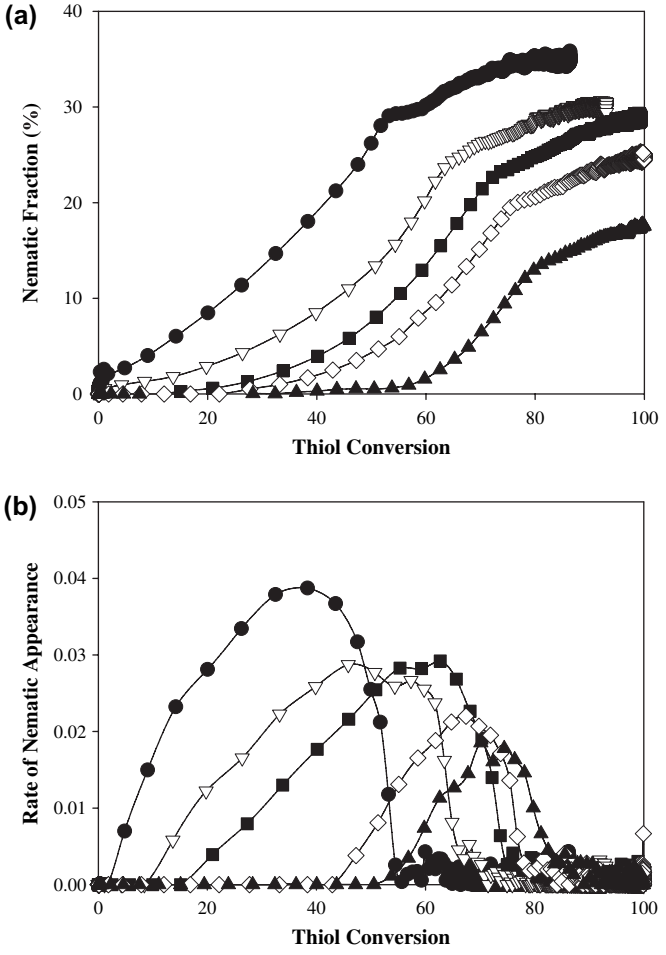

Fig. 6. Liquid crystal phase separation in thiol–ene HPDLC formulations containing mixtures of TATATO and diallyl ether. (a) Evolution of nematic fraction (%) and (b) rate of nematic appearance versus thiol conversion for the polymerization of HPDLC formulations containing TATATO (●), 75:25 TATATO/diallyl ether (▽), 50:50 TATATO/diallyl ether (■), 25:75 TATATO/diallyl ether (◇), and diallyl ether (▲).

decreases from 35% in thiol–TATATO HPDLC systems to 18% in thiol–diallyl ether HPDLCs. The evolution of LC phase separation as a function of monomer conversion is also dependent on the concentration of TATATO. As TATATO concentration decreases, the conversion at which the nematic LC begins to appear is increased. The initial slope of the nematic fraction versus conversion also decreases with decreasing TATATO concentration, indicating changes in LC demixing kinetics.

Fig. 6b more clearly illustrates the LC demixing kinetics of TATATO/diallyl ether systems, by plotting the rate of nematic appearance versus thiol conversion. The rate of nematic appearance is useful in correlating events in polymer evolution, such as gel point, to LC phase separation. The onset of LC phase separation is the point at which the rate of nematic appearance becomes greater than zero. The rate of nematic appearance for thiol–TATATO HPDLCs deviates from zero at very low conversion, indicating a nearly instantaneous onset of LC phase separation. As TATATO concentration is decreased in mixtures with diallyl ether, the onset of LC phase

separation is delayed to higher thiol conversion. In terms of the LC demixing kinetics, thiol–TATATO systems have the fastest rate of nematic appearance. Decreasing TATATO concentration decreases both the initial rate of nematic appearance and also the maximum rate of nematic appearance. Interestingly, the maximum in the rate of nematic appearance of these formulations occurs at the gel point conversion of the thiol–ene system.

Previous examination of LC phase separation in thiol–allyl ether HPDLCs has shown that the nematic fraction and rate of nematic appearance decrease with increased polymerization rate and/or decreased gel point conversion [15]. As shown in Fig. 6a and b, while increasing TATATO concentration increases the polymerization rate, it also increases the nematic fraction and rate of nematic appearance. Another factor that could influence the faster phase separation is the solubility of the LC in the ene monomer. The results of Fig. 6a and b indicate that BL037 liquid crystal is less soluble in TATATO than diallyl ether. In other words, the thiol–TATATO HPDLC formulation containing 27 wt% BL037 is just above the bimodal phase transition in the phase diagram for this system. Even with low monomer conversion, the equilibrium of the system is disturbed causing the system to shift into the two-phase region of the phase diagram. In the formation of HPDLCs, the immediate onset of LC phase separation leads to the dispersion of LC droplets throughout the polymer and LC lamellae. The poor definition of the polymer and LC lamellae reduces the refractive index mismatch, causing thiol-TATATO HPDLC reflection gratings to have DE of only 10%.

The interplay between LC solubility, polymerization rate, and HPDLC performance can be further understand by comparing mixtures of trithiol with TATATO and diallyl ether. Fig. 7a plots the transmission spectra of HPDLC reflection gratings containing diallyl ether, a 50:50 mixture of diallyl ether and TATATO, and TATATO. Reflection gratings based on diallyl ether monomer have poor baseline transmission but allow only 25% transmission at 540 nm. Reflection gratings based on TATATO have excellent baseline transmission, but poor reflection notch depth. Reflection gratings containing 50% TATATO and 50% diallyl ether maintain a great degree of the contribution of the baseline transmission of TATATO systems and a large degree of the reflection notch depth inherent in diallyl ether systems. This effect is further illustrated in Fig. 7b by examining DE and baseline transmission over a wide range of TATATO concentration. Clearly, increasing concentration of TATATO increases the baseline transmission of HPDLCs. Increasing TATATO concentration up to 50% increases DE in thiol–ene HPDLCs. The depth of the reflection notch begins to decrease at TATATO concentration greater than 50%, decreasing overall DE. HPDLC formulations containing a 50:50 mixture of TATATO and diallyl ether appear to optimize the DE of these systems by combining the desirable aspects of both ene monomers.

Further understanding regarding the improvement of optical properties and DE of HPDLCs through combination of both TATATO and diallyl ether is obtained upon examination of the polymer/LC morphology. Fig. 8 compares the

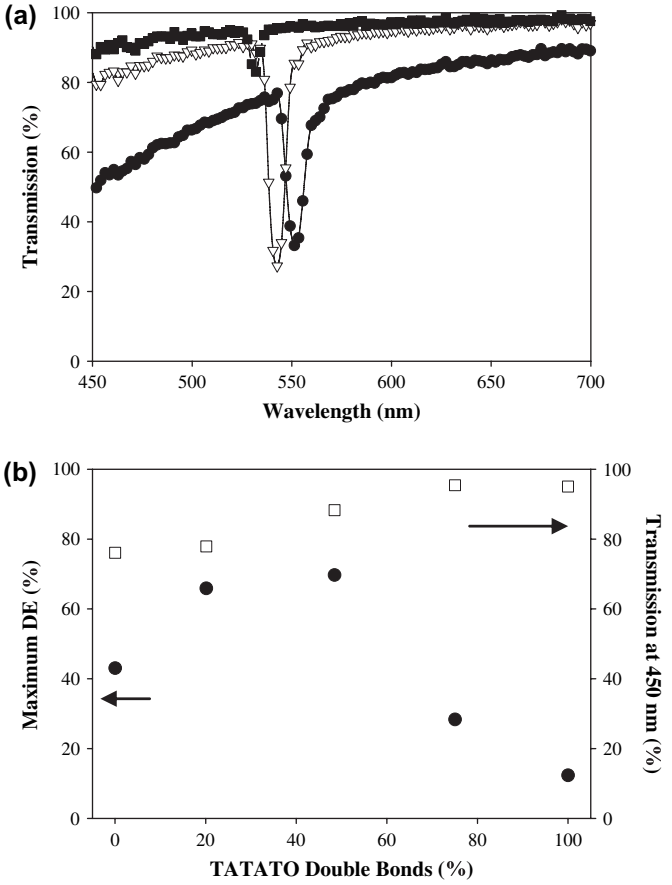

Fig. 7. HPDLC reflection gratings based on thiol–ene polymerization of TATATO and diallyl ether. (a) Transmission spectra of HPDLC reflection gratings based on polymerization of trithiol with TATATO (■), 50:50 TATATO/diallyl ether (▽), and diallyl ether (●) and (b) maximum DE (%) (●) and transmission at 450 nm (%) (□) for HPDLC reflection gratings containing 0–100% TATATO double bonds. Laser intensity – 60 mW/cm^2.

morphology of an HPDLC reflection grating made from the 50:50 mixture of TATATO and diallyl ether (Fig. 8a) to that of an HPDLC reflection grating based completely on TATATO (Fig. 8b). Decreasing the TATATO concentration increases LC droplet size from 25 nm to 60 nm. HPDLC reflection gratings based on the polymerization of a thiol with a 50:50 mixture of TATATO and diallyl ether have very few LC droplets in the polymer regions. Once again, the morphology of thiol–TATATO HPDLCs exhibits very poor lamellae definition. Therefore, mixing diallyl ether into thiol–TATATO HPDLCs increases grating definition and enhances DE.

Another critical parameter governing the application of HPDLC materials is switching voltage (SV). The impact of TATATO on SV in HPDLC reflection gratings is shown in Fig. 9, a plot of DE against applied voltage for thiol–ene mixtures of TATATO and diallyl ether. As TATATO concentration increases, the voltage necessary to switch the grating off increases from 9 V/μm in thiol–diallyl ether HPDLCs to nearly of 27 V/μm in thiol–TATATO HPDLCs. The SV of PDLC systems is dependent on LC droplet size and aspect ratio. As can be seen in the morphology shown in Fig. 8, these HPDLCs yield spherical droplets and have similar aspect ratios.

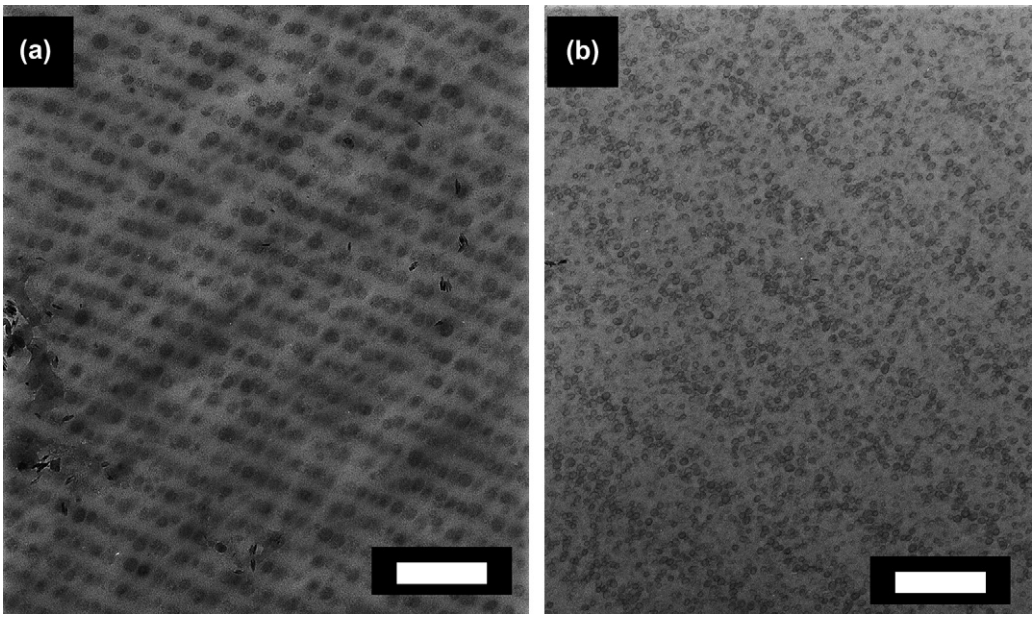

Fig. 8. TEM examination of polymer/LC morphology in HPDLC reflection gratings based on polymerization of trithiol with (a) 50:50 TATATO/diallyl ether, and (b) TATATO. Scale bar is 500 nm.

Therefore, the reduction of LC droplet size in HPDLCs with increasing TATATO concentration causes the switching voltage to also be directly dependent on TATATO concentration. The optimal concentration of TATATO for optical performance, 50%, has a switching voltage of 11 V/μm.

The DE of HPDLC reflection gratings based on thiol–TATATO–diallyl ether is comparable to the DE of HPDLC reflection gratings based on NOA65. NOA65 is a proprietary mixture of trithiol and a tetrafunctional urethane allyl ether that has commonly been used in PDLC systems [28]. In light of the results of this work, the performance of NOA65 based HPDLCs could be further enhanced with the addition of TATATO. Fig. 10 compares the transmission spectra of HPDLC reflection gratings based on the polymerization of NOA65 and NOA65 with 2 wt% TATATO. Adding only 2 wt% TATATO to HPDLC reflection gratings based on NOA65 further increases both baseline transmission and DE. In comparison to the NOA65 HPDLC, the NOA65–TATATO HPDLC increases baseline transmission at 450 nm by nearly 10% and increases overall DE by 7%, to nearly of 80%.

The performance enhancement with the addition of TATATO to NOA65 HPDLCs is once again based on changes in morphology. Fig. 11 compares micrographs of NOA65 based HPDLCs as characterized by TEM. NOA65 HPDLCs (Fig. 11a) have LC droplet size around 60 nm and well-defined grating structure. As shown in Fig. 11b, adding 2 wt% TATATO monomer decreases LC droplet size to 40 nm. The significant reduction in LC droplet size is the source of the

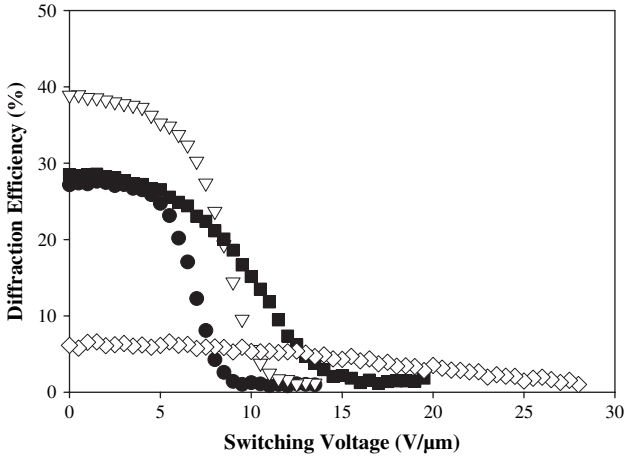

Fig. 9. Diffraction efficiency (%) versus switching voltage (V/μm) for HPDLC reflection gratings based on polymerization of trithiol with 50:50 TATATO/diallyl ether (▽), 75:25 TATATO/diallyl ether (■), diallyl ether (●), and TATATO (◇).

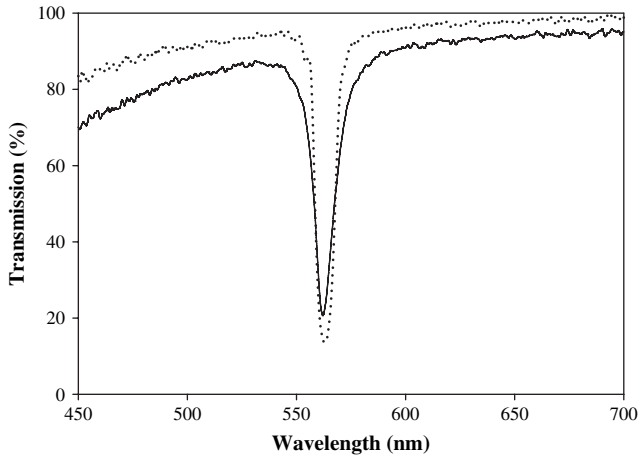

Fig. 10. Transmission spectra of HPDLC reflection gratings based on polymerization of NOA65 (—) and NOA65 + 2 wt% TATATO (···) at 60 mW/cm^2.

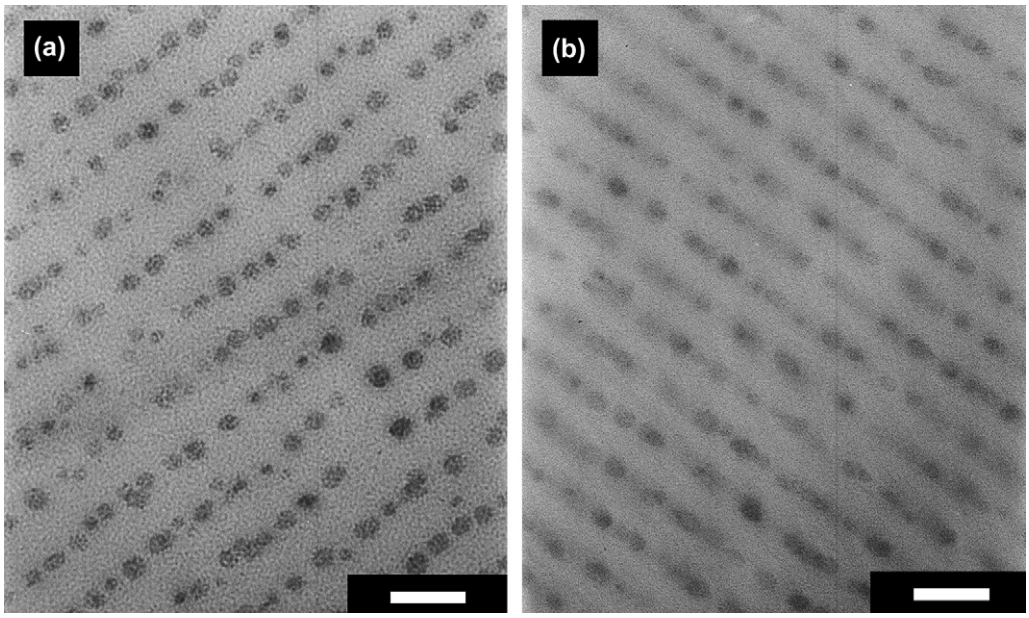

Fig. 11. TEM examination of polymer/LC morphology in HPDLC reflection gratings based on (a) NOA65 and (b) NOA65 and 2 wt% TATATO. Scale bar is 200 nm.

10% increase in baseline transmission and 7% increase in overall DE.

4. Conclusion

Incorporating fast-reacting ene monomers such as tri(ethylene glycol) divinyl ether (divinyl ether) and triallyl isocyanurate (TATATO) increase the baseline transmission of thiol–ene based HPDLC reflection gratings as polymerization of these monomers is two times faster than allyl ether monomer of equivalent functionality. The influence of TATATO on polymerization rate reduces LC droplet size to approximately 25 nm enabling 90% transmission at 450 nm. Despite the significant impact on baseline transmission, the DE of HPDLCs based solely on TATATO is only 10%, due to poorly defined HPDLC morphology. This poor morphology is caused by limited LC solubility in TATATO monomer that significantly increases liquid–liquid demixing. The increase in liquid crystal phase separation leads to the formation of a large number of LC droplets in the polymer lamellae and limited DE. Mixing TATATO into other HPDLC formulations, such as those based on trimethylolpropane diallyl ether (diallyl ether), reduces the rate of liquid–liquid demixing to enable the generation of well-defined grating structure. HPDLC reflection gratings containing a 50:50 mixture of TATATO and diallyl ether have a DE of nearly 70%, which approaches that of previously examined NOA65 HPDLCs. Introducing 2 wt% TATATO to HPDLC formulations containing NOA65 improves the optical performance of NOA65-based HPDLCs by reducing LC droplet size from 60 nm to 40 nm. In comparison to HPDLCs base on NOA65, the performance of HPDLC reflection gratings containing NOA65 and TATATO has a 10% increase in transmission at 450 nm and a 7% increase in DE.

Acknowledgement

The authors would like to acknowledge financial support from AFOSR, AFRL/ML, and the National Science Foundation (CBET-0328231).

References

[1] Bunning TJ, Natarajan LV, Tondiglia VP, Sutherland RL. Annu Rev Mater Sci 2000;30:83–115.
[2] Sutherland RL, Natarajan LV, Bunning TJ, Tondiglia VP. Switchable holographic polymer-dispersed liquid crystals. In: Nalwa HS, editor. Handbook of advanced electronic and photonic materials and devices. Liquid crystals, display and laser materials, vol. 7. San Diego, CA: Academic Press; 2001. p. 67–103.
[3] Pogue RT, Sutherland RL, Schmitt MG, Natarajan LV, Siwecki SA, Tondiglia VP, et al. Appl Spectrosc 2000;54(1):12A–28.
[4] Crawford GP. Opt Photonics News 2003;14:54.
[5] Fouassier J-P. Photoinitiation, photopolymerization and photocuring: fundamentals and applications. Cincinnati: Hanser/Gardner; 1995.
[6] Odian G. Principles of polymerization. 4th ed. New York: John Wiley and Sons; 2004.
[7] Natarajan LV, Shepherd CK, Brandelik DM, Sutherland RL, Chandra S, Tondiglia VP, et al. Chem Mater 2003;15(12):2477–84.
[8] Klosterman AM, Pogue RT, Schmitt MG, Natarajan LV, Tondiglia VP, Tomlin D, et al. MRS Proc 1999;559:129–34.
[9] Natarajan LV. Personal correspondence.
[10] Natarajan LV, Brown DP, Wofford JM, Tondiglia VP, Sutherland RL, Lloyd PF, et al. Polymer 2006;47(12):4411–20.
[11] White TJ, Natarajan LV, Tondiglia VP, Lloyd PF, Bunning TJ, Guymon CA. Macromolecules 2007;40:1121.
[12] Norland Products.
[13] Drzaic P. Liquid crystal dispersions. Singapore: World Scientific Publishing; 1995.
[14] Burget D, Mallein C, Fouassier JP. Polymer 2004;45(19):6561–7.
[15] White TJ, Natarajan LV, Tondiglia VP, Bunning TJ, Guymon CA. Macromolecules 2007;40:1112.

[16] Morgan CR, Magnotta F, Ketley AD. J Polym Sci Part A Polym Chem 1977;15(3):627.
[17] Jacobine AF. Radiat Curing Polym Sci Technol 1993;3:219.
[18] Hoyle CE, Lee TY, Roper T. J Polym Sci Part A Polym Chem 2004;42:5301.
[19] Jacobine AF, Woods JG, Rakas MA. Polymer dispersed liquid crystals in electron-rich alkene-thiol polymers. US: WO 9,425,508; 1994.
[20] Vaz NA, Smith GW. Liquid crystal droplets dispersed in thin films of UV-curable polymers. US: 4,728,547; 1988.
[21] EMD Chemical.
[22] White TJ, Liechty WB, Natarajan LV, Tondiglia VP, Bunning TJ, Guymon CA. Polymer 2006;47:2289.
[23] Babkov LM, Gnatyuk II , Trukhachev SV. J Mol Struct 2005;744–747:425.
[24] Bhargava R, Wang SQ, Koenig JL. Macromolecules 1999;32:8982–8.
[25] Bhargava R, Wang SQ, Koenig JL. Macromolecules 1999;32:8989–95.
[26] Klosterman J, Natarajan LV, Tondiglia VP, Sutherland RL, White TJ, Guymon CA, et al. Polymer 2004;45(21):7213–8.
[27] For more information regarding the use of RTIR to monitor liquid crystal phase separation, see Refs. [11,15,23–25].
[28] Senyurt AF, Warren G, Whitehead JB, Hoyle CE. Polymer 2006;47:2741.